

WIDE-BANDWIDTH, HIGH FRAME RATE ELECTRICAL IMPEDANCE TOMOGRAPHY / SPECTROSCOPY

A Code Division Multiplexing (CDM) Approach

A. L. McEwan, D. S. Holder

Department of Medical Physics and Bioengineering, University College London, Gower St London, UK

J. Tapson

Department of Electrical Engineering, University of Cape Town, Cape Town, South Africa

A. van Schaik

School of Electrical and Information Engineering, University of Sydney, Sydney, Australia

Keywords: Electrical impedance tomography, electrical impedance spectroscopy, bioimpedance measurement, code division multiplexing.

Abstract: We present a proposal and proof-of-concept, experimental results for a new type of electrical impedance tomography / spectroscopy system that makes use of code division multiplexing to achieve two important technological advances. Assigning each channel an orthogonal code allow all the impedance measurements to be made simultaneously in time, thereby increasing the frame rate; and the use of pseudorandom input signals allows a very wide range of frequencies to be sampled simultaneously in each channel.

1 INTRODUCTION

Electrical impedance tomography (EIT), in which a volume is probed non-invasively by injecting currents (or magnetic fields) and measuring the electrical potential or magnetic fields at the periphery, has been used for physiological imaging for three decades (Holder, 2005). Its applicability in industrial situations, in which it is called process tomography, was recognized in the early 1980's (Beck and Williams, 1996), leading to a considerable investment in research into hardware, software, and reconstruction algorithms (West, 2002). More recently, there has been a growing interest in obtaining material contrast in the images by discriminating on the basis of the frequency response of impedance; this is electrical impedance spectroscopy (EIS) (Brown, 2001). The combination of the two methods is generally called EITS.

In the standard implementation of EIT, the complex impedance is measured in terms of resistance and capacitance. A ring of (usually 8 or 16) electrodes is placed around the volume to be imaged (generally, a single plane or slice is imaged,

and volumes reconstructed from a number of planes; hence the use of the word tomography). A current is injected through a pair of the electrodes, and the resulting electrical potentials measured at all of the other electrodes. The signals are separated into a resistive and a capacitive signal, either by measuring the complex impedance directly, or by using separate ohmic and capacitive electrodes.

If the frequency of the injected current is swept through a range, or stepped through a set of fixed frequencies, the spectral response may also be obtained. The current excitation is then switched to a new pair of electrodes, and a new data set acquired. When all the desired combinations have been measured, a reconstruction algorithm is used to produce an approximation of the distribution of material within the image plane, based on its impedance (in EIT) or impedance spectrum (in EITS). The reconstruction of EITS images is an area of active research, and many different methods are available (Polydorides and Lionheart, 2002).

There are a number of standard patterns of excitation and measurement in EITS. The most commonplace is that adjacent pairs of electrodes are

used to inject current, and potentials are measured at all other adjacent pairs. This method has the advantage that once a pair of electrodes has been used for current injection, and its response at all other electrodes measured, it is thereafter redundant to measure potentials at that pair and therefore the number of measurements required is reduced. Regardless of the pattern used, a single frame of EIT data requires a great many measurements (the adjacent-pair method requires $k = n \times (n-1)$ measurements for n electrodes); and this number must be multiplied by the number of frequency points required.

Taking a frame of EIT data using sequential measurements – so-called time-division multiplexed or TDM measurements) is slow, so that frame rates in excess of 100 frames/second are extremely difficult to achieve. Wilkinson and co-workers (2003) have optimized the TDM process to a very high degree, achieving frames rates of up to 1000 frames/s; but most laboratory and commercial systems operate at orders of magnitude slower than this. EITS systems are slower still, with frame rates of 13 seconds/frame achievable with a frequency range of 20 Hz – 128 kHz in current systems (McEwan et al., 2006). A basic constraint in EITS frame rate is imposed by the lower limit of spectral bandwidth; for example, if the impedance at 20Hz is required, the frame rate per second will be limited to $20/k$, where k is the number of sequential measurements required per frame; even this limit implies sampling only a single cycle of the lowest frequency per measurement, which is somewhat difficult to achieve in practice.

A method which presents itself for increasing the frame rate is simultaneously to inject currents which are modulated to be mathematically orthogonal, so that their contributions to the potential at any electrode can be separated by demodulation. For example, if a current of frequency f_1 is injected at one pair of electrodes, and a current of frequency f_2 at a second pair, then the potential across a third pair of electrodes can be separated into a component due to f_1 and a component due to f_2 by synchronously demodulating with those frequencies. The complex components of impedance can be extracted by in-phase and quadrature synchronous demodulation. This is called frequency-division multiplexed (FDM) EIT.

FDM EIT appears to have been developed simultaneously by Tapson and colleagues (Tapson & Teague, 2002), and Zimmermann and colleagues (Zimmermann et al., 2002); although as both developments were patented and not published in the

scientific literature, public domain details are few (Teague, 2002).

A number of problems are encountered in FDM EIT as a consequence of accommodating simultaneous current injection and voltage measurement on the same electrode. If the current and voltage form part of the same impedance calculation, this comprises a two-terminal impedance measurement; whereas it is generally considered that a four-terminal measurement is required to avoid the problem of inadvertently including the contact or terminal resistance in the specimen resistance. If the current and voltage form part of a separate calculation, then this problem is avoided.

A second issue is that the current through any terminal must be a sum of orthogonal component currents, and equal and opposite components must flow through some other terminal. Ensuring that the net current due to each component is zero is electronically complicated, and has not been attempted in any of the known FDM EIT systems. These systems have generally avoided these problems by using separate sets of current injection and voltage measurement electrodes, although this has the disadvantage that twice the number of electrodes are required to obtain the same resolution. Data comparing the resolution of FDM and TDM systems is scarce (Goldswain & Tapson, 2006), but those results as well as unpublished work (Elliot, 2006) suggest that FDM systems are at least as accurate as TDM systems.

In this paper we present a new approach to EITS instrumentation. We make use of Code-Division Multiplexing (CDM) to inject orthogonal currents simultaneously, and to demodulate the resulting potentials. This has an enormous advantage over FDM and TDM techniques, in that it is possible to sample at multiple frequencies simultaneously while sampling multiple physical channels. The result is a system in which wide-bandwidth multi-electrode spectroscopy can be performed in times equivalent to that taken for single measurements in current EITS systems. The CDM process can be seen as a natural extension of FDM EIT, and many of the same issues apply. In order to deal with the problem of sharing electrodes between multiple measurement channels, we have developed a simple current injection arrangement at the electrode, based on high-frequency transformers, which guarantees a net zero current flow for each orthogonal component. The new system is described in detail in the following sections.

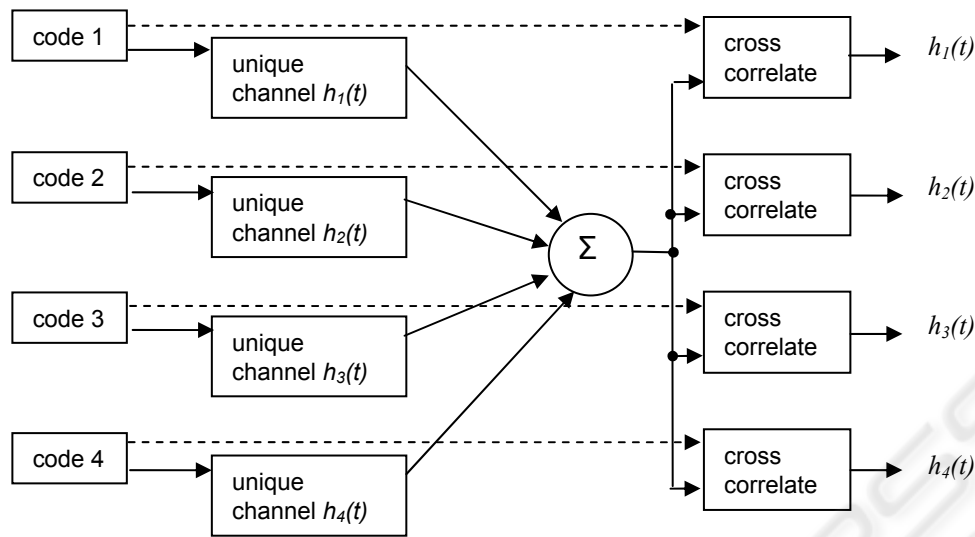


Figure 1: The code-division multiplexing principle. Each unique channel in the measurement system is stimulated using a driving signal modulated with a unique binary pseudorandom (PRN) code. The channels are then either deliberately or inadvertently mixed together. At the receivers, the contribution due to each channel is recovered by cross-correlating the signal at the receiver, and a copy of the driving signal containing the channel's characteristic code. If the codes are orthogonal or near-orthogonal, there should be complete separation of components. Serendipitously, the cross-correlation produces the impulse response of the channel (see Equations 1-6).

2 CODE-DIVISION MULTIPLEXING OF EIT CHANNELS

The principle of CDM is that the signal through a particular channel is modulated using a unique binary digital code (see Figure 1). A receiver which is receiving several channels can separate the data for each channel by demodulating using a copy of the same code. There are a number of different codes which may be used. The basic requirements are that there should be at least one code per channel; that the codes should be orthogonal, or nearly so; and that the autocorrelation functions of the codes should be flat with a single sharp peak (in the ideal case, approximating a delta function) (Sarwate & Pursley, 1980). The codes which we have used in this work are called Gold codes, and are used in the Global Positioning System (GPS) to encode the signals from the GPS satellite constellation; these signals can then be unambiguously demodulated by a terrestrial GPS receiver equipped with copies of the codes (Parkinson & Spilker, 1996). The codes are bit sequences which appear to be random, but in fact are deterministically generated, usually by means of a modulo-addition of bits in a shift register. Codes of this type are generally referred to as pseudorandom

noise (PRN) sequences, as they appear to be random and have the characteristics of noise.

In this system, we achieve two important goals using CDM. Firstly, the use of CDM allows us to take measurements over all the channels simultaneously. Secondly, the spectral characteristics of the CDM input signal effectively interrogate the sample over a wide range of frequencies, and the output signals can be transformed to produce a spectrum, giving us simultaneous wide-band spectroscopy on all channels. The following two sections explain these features.

2.1 The Use of Code Division Multiplexing to Provide Simultaneous Measurement

The use of CDM in an EIT system is shown conceptually in Figure 1. We use the PRN codes as the input stimulus to a system. The system has a unique channel for each input, but unfortunately all the channel outputs are combined linearly, so that the unique response for each channel is not explicitly available.

When we perform a cross-correlation R_{IO} between the unique input signals I_n and the combined output signal O_n , we are calculating:

$$R_{I_1 O}(m) = \frac{1}{N} \sum_{n=0}^{N-1} I_{1n} O_{n-m} \quad (1)$$

where N is the epoch length of the PRN (nominally, 1023 bits, or the equivalent number of samples).

The output at any time k can be stated as the sum of the convolution of the impulse responses for the channels and the respective inputs:

$$O_k = \sum_{i=0}^k I_{1i} h_{1(k-i)} + \sum_{i=0}^k I_{2i} h_{2(k-i)} + \sum_{i=0}^k I_{3i} h_{3(k-i)} + \dots \quad (2)$$

If we substitute this into the cross-correlation, say for I_1 and the output:

$$\begin{aligned} R_{I_1 O}(m) &= \frac{1}{N} \sum_{n=0}^{N-1} I_{1n} \left[\sum_{i=0}^{n-m} I_{1i} h_{1(n-m-i)} + \right. \\ &\quad \left. \sum_{i=0}^{n-m} I_{2i} h_{2(n-m-i)} + \sum_{i=0}^{n-m} I_{3i} h_{3(n-m-i)} + \dots \right] \\ &= \frac{1}{N} \sum_{n=0}^{N-1} I_{1n} \sum_{i=0}^{n-m} I_{1i} h_{1(n-m-i)} + \\ &\quad \frac{1}{N} \sum_{n=0}^{N-1} I_{1n} \sum_{i=0}^{n-m} I_{2i} h_{2(n-m-i)} + \dots \\ &= \frac{1}{N} \sum_{n=0}^{N-1} \sum_{i=0}^{n-m} I_{1n} I_{1i} h_{1(n-m-i)} + \\ &\quad \frac{1}{N} \sum_{n=0}^{N-1} \sum_{i=0}^{n-m} I_{1n} I_{2i} h_{2(n-m-i)} + \dots \end{aligned} \quad (3)$$

Given that:

$$\sum_{i=0}^k I_{1i} h_{1(k-i)} = \sum_{i=0}^k I_{1(k-i)} h_{1k} \quad (4)$$

We can rearrange as follows:

$$\begin{aligned} R_{I_1 O}(m) &= \frac{1}{N} \sum_{n=0}^{N-1} \sum_{i=0}^{n-m} I_{1n} I_{1(n-m-i)} h_{1i} + \\ &\quad \frac{1}{N} \sum_{n=0}^{N-1} \sum_{i=0}^{n-m} I_{1n} I_{2(n-m-i)} h_{2i} + \dots \\ &= \sum_{i=0}^{n-m} R_{I_1 I_1}(m-i) h_{1i} + \\ &\quad \sum_{i=0}^{n-m} R_{I_1 I_2}(m-i) h_{1i} + \dots \\ &= R_{I_1 I_1} * h_1 \\ &= h_1(m) \end{aligned} \quad (5)$$

The cross-correlation terms (those R_{II} terms with non-identical indices for I) will sum to zero, because different Gold codes are effectively uncorrelated; so only the first correlation is non-zero. In continuous terms:

$$\begin{aligned} R_{I_1 O}(t) &= R_{I_1 I_1}(t) * h_1(t) \\ &= \delta(t) * h_1(t) \\ &= h_1(t) \end{aligned} \quad (6)$$

The output of the cross-correlation is the impulse response of the channel, which represents the time-domain transform of the information we want.

2.2 Hardware Implementation

Part of the proposed hardware implementation is shown on the following page, with a number of elements not shown to improve clarity. We use transformer coupling of the drive currents to the EIT electrodes in order to ensure matched source and sink currents. There is a resistor in each transformer secondary, to allow direct measurement of the current in the secondary. The way in which the system works is as follows. The microprocessor system outputs currents which are modulated in polarity by the Gold codes (using push-pull drive from two port pins, with a series resistor for current limiting). Each of the eight transformer secondaries is connected to a pair of electrodes, so that each electrode is connected to the high side of one secondary and the low side of another.

In principle, the current between terminals T1 and T2 should have a fixed amplitude, modulated in polarity by Code 1. In practice, we measure this current by sampling the voltage at the points V_1 and VT_1 , and dividing the difference by the resistor value.

We can then calculate the impulse response for the voltage between T_4 and T_5 , with respect to the current between T_1 and T_2 , by cross-correlating the voltages ($V_1 - VT_1$) and ($V_5 - V_4$); and so on.

2.3 Spectral Response of the CDM System

As discussed earlier, PRN sequences have the appearance of noise, and like uniformly distributed white noise, their spectrum is flat within the limits of bandwidth. They are also delta-correlated; that is to say, their autocorrelation function consists of a Dirac delta function at the origin. This is the basis of their usefulness in demodulation, as shown above. From (6) above we see that the input-output cross-correlation function of a channel in the system pro-

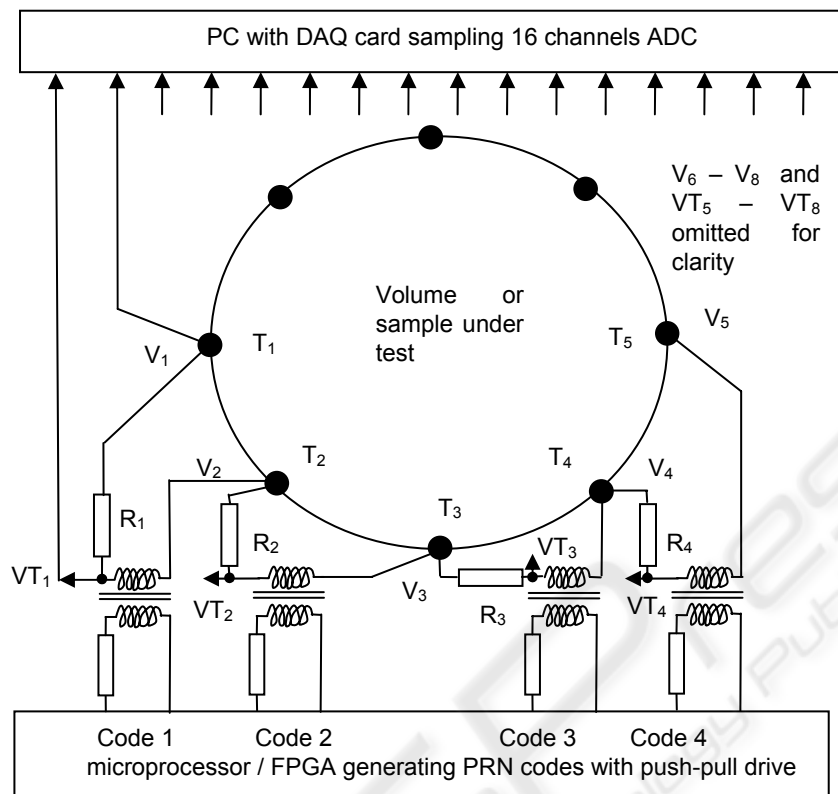


Figure 2: Block diagram of the proposed system, showing multiple electrodes at which drive and reception of signals is combined. Transformer coupling allows inflowing and outflowing currents due to each code to be exactly balanced, as well as providing isolation for safety. The voltage across each ballast resistor gives the current due to that code (e.g. the current due to Code 3 is $I_3 = (VT_3 - V_3)/R_3$).

duces the transfer function $h(t)$ of the channel. If we take the Fourier transform of the cross-correlation function:

$$\begin{aligned}
 G(\omega) &= \int_{-\infty}^{\infty} R_{I,O}(t) e^{-j\omega t} dt \\
 &= \int_{-\infty}^{\infty} h(t) e^{-j\omega t} dt \\
 &= h(\omega)
 \end{aligned}
 \tag{7}$$

so, the Fourier transform of the cross-correlation function produces the frequency response of the channel; which is to say, the complex spectrum of the channel impedance.

3 PROOF OF CONCEPT – EXPERIMENTAL RESULTS

3.1 Method

In order to establish the workability of this concept, we require to demonstrate two methods:

- The feasibility of extracting wide-range, high resolution impedance measurements when driving the channels with PRN codes.
- The feasibility of simultaneously stimulating several channels and recovering the individual signals from the multiplexed signal by demodulation.

We have done this as a proof-of-concept by conducting an imaging experiment with an existing EITS system, using both the standard sinusoidal waveforms, and a new waveform based on the Gold code intended for CDM-EIT.

A serial, EITS system, the UCL Mk2.5, was reprogrammed with the 1st 1023-length code of a set of eight Gold codes. Only one code was used as the Mk2.5 is based on a single channel of the Sheffield Mk3.5 system multiplexed to 32 electrodes. In normal operation the Mk2.5 system measures the spectrum using a 2048-length composite waveform of 10 frequencies of equal amplitude, logarithmically spaced between 2kHz and 1MHz (McEwan et al., 2006; Wilson et al., 2001). The Gold code was sampled at 2samples/bit to meet the

Nyquist criteria with an additional zero bit added to ensure its length was 2^{12} . This is required by the matched filter which is performed by the system DSP processor. As the length of both test waveforms are the same, and the timing of the system clock (2MHz) was unchanged, they span the same frequency range of 2kHz-1MHz. For simplicity, and to ensure that the instrumentation did not saturate, the amplitude of the gold code waveform was set to the maximum of the composite waveform.

An often used test of an EITS system is its ability to produce images of an object in a tank filled with saline solution. Boundary voltage measurements are collected from the tank with and without the object (so-called *perturbation* and *reference* frames). These two sets of data are subtracted then used with a reconstruction algorithm to produce a *time-difference* image. In keeping with previous EITS measurements we chose to use a piece of banana as our object, as it changes impedance by over 100% between 2kHz and 1MHz (Yerworth et al., 2003). The saline solution's impedance will remain relatively unchanged over the same frequency range and hence it is possible to determine the spectrum of the object inside the tank from a sequence of images at the measured frequencies.

The tank was cylindrical, 10cm diameter, filled with 0.1% saline solution with 16 stainless steel electrodes in a ring. The test object was a cylinder of banana, 2 cm long and 1 cm in diameter. Image reconstruction was done using a linear solver (EIDORS) (Polydorides and Lionheart, 2002) and a 15,000 element FEM mesh of the tank.

3.1.1 Results

The spectra for the banana object were constructed by plotting the value of a pixel in the known position of the object, at 10 different frequencies.

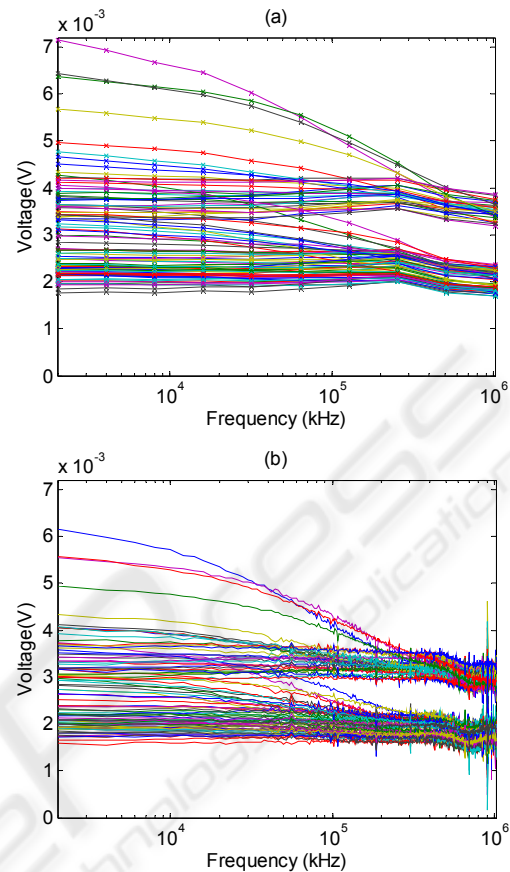


Figure 3: Comparison of boundary voltage measurements in a single frame. Each line is a different electrode combination measurement. Larger voltages occur when the voltage electrodes are near current-carrying electrodes. Combinations more sensitive to the perturbation show a greater change over frequency. Figure 3(a) shows a composite representation of the output of the standard 10 frequency system. Figure 3 (b) shows the output of the new system, using PRN codes for excitation and demodulation. It can be seen that the PRN codes provide the same response as the standard method, but with a much higher resolution in frequency.

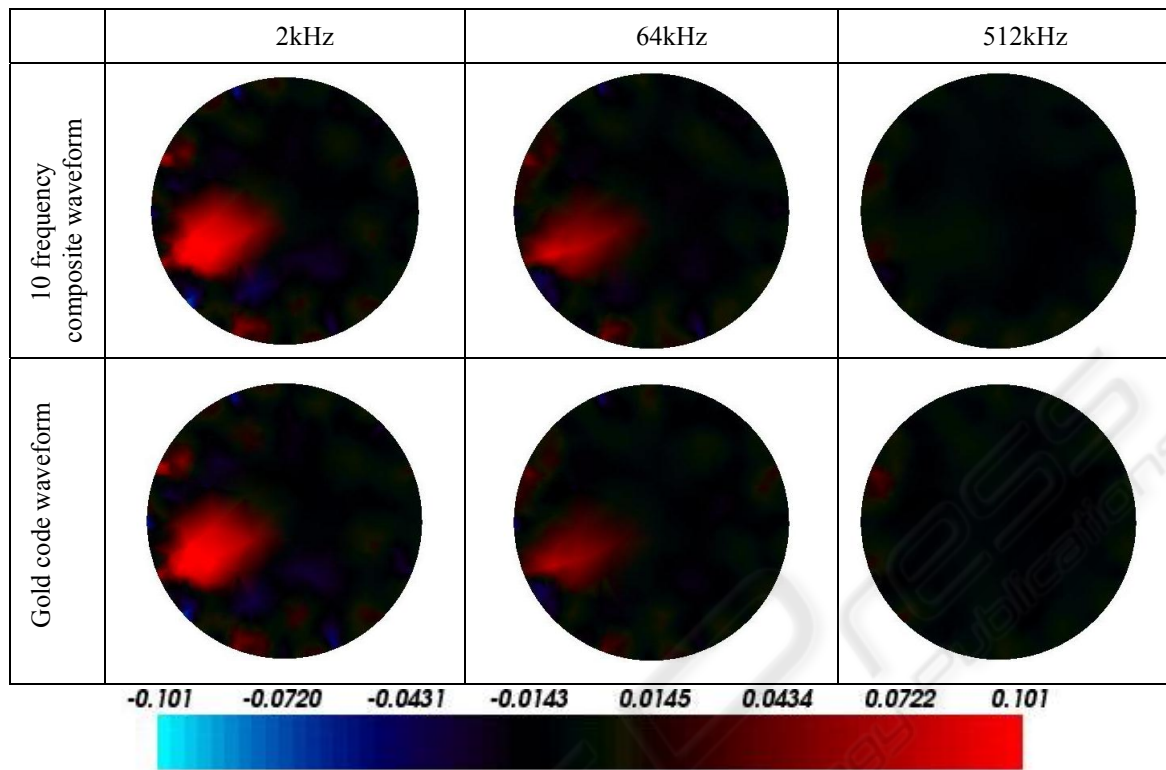


Figure 4: Time difference images collected at three frequencies using the two waveforms. As the frequency increases, the contrast (impedance difference) between perturbation and background decreases. It can be seen that the new PRN (Gold code) method offers the same resolution as the standard 10-frequency method, with the potential for significantly faster operation.

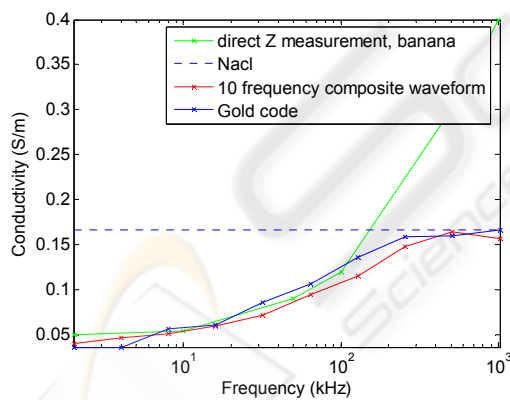


Figure 5: Spectra obtained from the data used in Figure 4. These spectra are similar to those that have been previously obtained from the Mk2.5 system. The new method produces a spectrum which is very similar to the standard method. Both EITS spectra deviate from a direct measurement at frequencies above 128kHz, for reasons explained below.

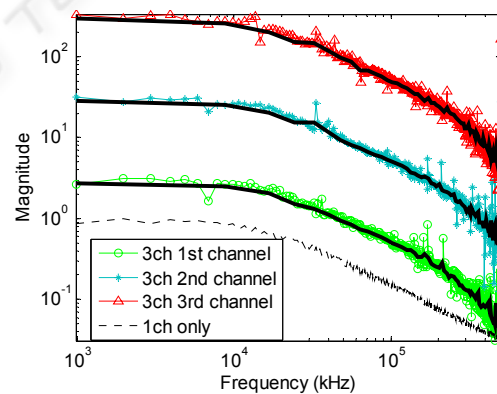


Figure 6: Spectral magnitude for three multiplexed channels, independently stimulated with PRN codes, mixed together on a single circuit impedance, and then demodulated. For clarity each channel has been multiplied by 10^x where x is the channel number. It can be seen that the multiplexed signals can be independently recovered after mixing, and are a good match (although noisier) to the single channel case. The thick black lines show a average spectra, possible due to the large number of frequencies available in this method.

4 DISCUSSION

The boundary voltages measurements using the two waveforms are similar, as shown in Figure 3. The PRN code voltage measurements are 1mV lower, due to the lower current per frequency component. As this is constant between the perturbation and reference frames, it is cancelled out in the subtraction process and is not apparent in the images. The PRN code boundary voltages appear to be noisier, particularly at higher frequencies. In practice these frequencies would be averaged together reducing the noise. The Mk2.5 EIT system has limited performance at frequencies above 128kHz due to the effect of 0.5m long unscreened cables. These are likely to be the cause of the increased noise seen in the PRN code spectra, a real effect which is not seen in the lower frequency resolution of the 10 frequency composite waveform. The 128kHz limit is also apparent in the spectra, which deviate from a direct impedance measurement above this frequency.

We have shown the feasibility of using PRN codes for EITS, both in extracting the system impulse response, and in terms of simultaneous excitation and demodulation. The images and extracted spectra are very similar to those obtained using the standard method, demonstrating the proof of the concept of using CDM waveforms for EIT acquisition. The primary advantage of greatly increased frequency resolution for the same acquisition time has been demonstrated. We are currently implementing a multiple source system which should lead to a system with two orders of magnitude increase in frame rate over the standard method, along with the improved frequency resolution demonstrated here.

ACKNOWLEDGEMENTS

Action Medical Research RTF 3110 and The University of Sydney International Visiting Research Fellowship 2007.

REFERENCES

- Beck, M.S. & Williams, R.A. (1996). Process tomography: a European innovation and its applications, *Meas. Sci. Technol.*, 7, 215–24.
- Brown, B.H. (2001). Medical impedance tomography and process impedance tomography: a brief review, *Meas. Sci. Technol.*, 12, 991-996.
- Elliot, J. (2006). *Electrical impedance tomography imaging of a hydrocyclone*, M.Sc thesis (University of Cape Town).
- Goldswain, G., & Tapson, J. (2006). Kernel ridge regression for volume fraction prediction in electrical impedance tomography, *Meas. Sci. Technol.*, 17, 2711-2720.
- Holder, D.S. (ed.) (2005). *Electrical Impedance Tomography: Methods, History and Applications*, Bristol and Philadelphia: IOP.
- McEwan, A., Romsauerova, A., Yerworth, R., Horesh, L., Bayford, R., & Holder, D. (2006). Design and calibration of a compact multi-frequency EIT system for acute stroke imaging, *Physiol. Meas.*, 27, S199-S210.
- Parkinson, B.W., & Spilker Jr., J.J. (1996). *Global Positioning System: Theory and Applications*, vol. 1, Am. Inst. Aeronautics and Astronautics Inc., Washington.
- Polydorides, N. & Lionheart W.R.B. (2002). A Matlab toolkit for three-dimensional electrical impedance tomography: a contribution to the Electrical Impedance and Diffuse Optical Reconstruction Software project, *Meas. Sci. Technol.*, 13, 1871-1883.
- Tapson, J., & Teague, G. (2002). *Method and Apparatus for Electrical Impedance Tomography*, SA Patent 2002/3689.
- Teague, G. (2002). *Mass Flow Measurement of Multi-Phase Mixtures by Means of Tomographic Techniques*, PhD thesis, (University of Cape Town). retrieved June 24, 2007 from <http://mysite.mweb.co.za/residents/jontapson/>
- Sarwate, D.V., & Pursley, M.B. (1980). Crosscorrelation properties of pseudorandom and related sequences, *Proc. IEEE*, 68, 593-619.
- West, R. (ed.) (2002). Special Feature: Process Tomography, *Meas. Sci. Technol.*, 13, 1799-1902.
- Wilkinson, A.J., Randall, E.W., Durrett, D., Naidoo, T. & Cilliers, J.J. (2003). The design of a 1000 frames per second ERT data capture system and calibration techniques employed. *Proc. 3rd World Congress on Industrial Process Tomography*, Banff, 504-509.
- Wilson, A.J., Milnes, P., Waterworth, A.R., Smallwood, R.H., & Brown, B.H. (2001). Mk3.5: a modular, multi-frequency successor to the Mk3a EIS/EIT system, *Physiol. Meas.*, 22, 49-54.
- Yerworth, R.J., Bayford, R.H., Brown, B., Milnes, P., Conway, M. & Holder, D.S. (2003). Electrical impedance tomography spectroscopy (EITS) for human head imaging, *Physiol. Meas.*, 24, 477-489.
- Zimmermann, E., Glaas, W., Verweerd, A., Tillmann, A., & Kemna, A. (2002). *Method and apparatus for rapid tomographic measurements of the electrical conductivity distribution of a sample*, German patent DE 102 38 824.